Agriculture, Ecosystems and Environment 400 (2026) 110258

Contents lists available at ScienceDirect

Agriculture, Ecosystems and Environment

journal homepage: www.elsevier.com/locate/agee

Spatiotemporal patterns of ammonia fluxes on temperate dairy farm production grassland (*Lolium perenne* L.)

Claudia C. Schwennen [a], Albert Tietema [a], Emiel E. van Loon [a], Klaus S. Larsen [b], Tamar Tulp [a], Bram Ebben [a], Roland Bol [a,c], S. Henrik Barmentlo [d,*]

[a] Department of Ecosystem and Landscape Dynamics, Institute for Biodiversity and Ecosystem Dynamics, University of Amsterdam, Science Park 904, Amsterdam 1090 GE, the Netherlands
[b] Department of Geosciences and Natural Resource Management, Copenhagen University, Rolighedsvej 23, Frederiksberg 1958, Denmark
[c] Agrosphere department, Institute of Bio, and Geosciences, Helmholtz Forschungszentrum Jülich, Wilhelm-Johnen-Straße, Jülich 52428, Germany
[d] Department of Environmental Biology, Institute of Environmental Sciences, Leiden University, Einsteinweg 2, Leiden 2333 CC, the Netherlands

ARTICLE INFO

Keywords:
Agriculture
Slurry manure
Artificial fertilizer
NH_3
Emission
Deposition

ABSTRACT

The nitrogen cycle is significantly altered by agricultural activities such as animal husbandry and fertilization, which can turn the landscape from a natural sink of ammonia (NH_3) to a net source. Ammonia fluxes at broader spatiotemporal scales have been well studied, however, smaller-scale, point source studies are needed to quantify atmosphere-biosphere nitrogen balances around individual agricultural sources such as extensively managed production grassland. The aim of this study was to quantify the spatiotemporal variation in NH_3 fluxes on dairy farm production grassland (*Lolium perenne* L.) throughout a full year. We focused on the dairy stable as a point emission source, as well as on the management practices (such as slurry application) performed by farmers. The temporal variation in NH_3 fluxes was assessed using novel automated dynamic flux chambers adapted for NH_3. Manual flux chambers were deployed to determine spatial variation. While fluxes did vary spatially, we found significant losses of NH_3 (99.6 %) during the growing and harvesting season (March to September). This was largely attributed to substantial emission rates directly after slurry application while net emission/deposition was close to zero during late-fall and winter. Overall, the net annual NH_3-N emission of this production grassland was 12 kg ha^{-1} y^{-1}. Post slurry application emissions were especially high during warm and dry weather conditions. Optimizing the timing of fertilization application according to local weather conditions can therefore serve as a management practice to limit NH_3 emission, benefitting both farmers and the natural environment.

1. Introduction

The natural biogeochemical nitrogen cycle is continuously altered by anthropogenic interference, causing the planetary boundary for biochemical flows to surpass the safe operating space (Richardson et al., 2023). This is because anthropogenic processes such as agriculture, industry and transport, constantly increase the emissions of atmospheric reactive nitrogen ('N_r') (Stevens, 2019; Zhang et al., 2021). Once in the atmosphere, N_r is transported downwind from its source and returned to the biosphere through atmospheric deposition (Flechard et al., 2013; Zhang et al., 2021), which can cause severe environmental issues when in excess (Zhang et al., 2021).

In the Netherlands, the emission of ammonia (NH_3) is the main contributor to excess N_r deposition, and the dairy sector is the dominant source (Feest et al., 2014; Stokstad, 2019). In 2022, over 23 % of the Netherlands was used for production grassland (Central Statistics Office (CBS) (CBS), 2023), which theoretically could act as NH_3 sinks, but activities as animal husbandry and fertilization can trigger NH_3 emissions causing (production) grasslands to behave as NH_3 sources instead (David et al., 2009; Flechard et al., 2013). It is estimated that about 60 % of Dutch nature areas is exposed to nitrogen deposition above critical loads (Post et al., 2020). Such emission and deposition dynamics at broader spatiotemporal scales have been thoroughly assessed in previous studies (Flechard et al., 2013), however, the underlying assumption in the methods that are used at these scales include measuring over a uniform surface area (Fang et al., 2020). Applying this approach at point sources, which might be distributed over the study area (Wong, 2018), may lead to biases and uncertainties in flux measurements (Fang et al.,

* Corresponding author.
E-mail address: s.h.barmentlo@cml.leidenuniv.nl (S.H. Barmentlo).

https://doi.org/10.1016/j.agee.2026.110258
Received 29 January 2025; Received in revised form 10 December 2025; Accepted 19 January 2026
Available online 24 January 2026
0167-8809/© 2026 The Authors. Published by Elsevier B.V. This is an open access article under the CC BY license (http://creativecommons.org/licenses/by/4.0/).

2020). In order to assess the complexity associated with the mechanisms involved in N flows around individual point sources and to accurately quantify N balances or net budgets, small-scale studies targeted specifically at point sources are needed (Oenema et al., 2015; Einarsson et al., 2018).

Flux chambers are commonly used to study spatial and temporal patterns at the small scale (Heinemeyer et al., 2013; Hoffmann et al., 2017), however, the use of flux chambers to study NH_3 fluxes has been limited due to the nature of the gas. Ammonia can easily dissolve in water, making it difficult to use conventional chambers due to the formation of water droplets (i.e. condensation) when the chamber is closed (Sintermann et al., 2012; Van Damme et al., 2015; Delon et al., 2017). Here we make use of automatic (stationary and automated) and manual flux chambers that are newly designed to specifically quantify NH_3 fluxes. We use this equipment to elucidate the knowledge gap of sink-source dynamics of NH_3 caused by dairy farming. In this study, we aim to quantify the annual NH_3 budget (i.e. the net emission or deposition) on production grassland close to a dairy stable in the north of the Netherlands. This not only allows for identifying source-sink dynamics in relation to the livestock stable as a point source, but also in relation to the agricultural management practices (hereafter: management practices) conducted throughout the harvesting season. Moreover, it allows for determining the spatiotemporal variation in NH_3 fluxes of the production grassland. We hypothesize that fluxes will vary both spatially, as local atmospheric concentrations gradients relative to the stable can be steep (Tulp et al., 2024), and temporally, as ammonia emissions are strongly driven by seasonality (Flechard et al., 2010; Todd et al., 2011). To address these questions, three automatic flux chambers were deployed to measure temporal fluxes during a full year, whereas spatial fluxes were assessed by conducting manual flux measurements along spatial transects across the production grassland.

2. Methods

2.1. Site description

The experiment was set up (see 2.2) at a commercial dairy farm located in the province of Friesland in the Netherlands where no other livestock farms or other interfering N_r sources were present within a radius of 1 km (Supplement, Fig. S1). Additionally, the landscape is flat so that atmospheric transport by ammonia is not hindered by obstruction (see also Tulp et al., 2024). With a temperate maritime climate, the average air temperature in 2022 was 11.3 °C with a total of 766 mm of rain throughout the year (measured with a meteorological station on site, see 2.2). The farm covers an area of approximately 100 ha with clay-rich soils, comprised of 55 ha production grassland (*Lolium perenne* L.) and 17 ha silage maize (*Zea mays* L.), while some smaller plots are used for potato (*Solanum tuberosum* L.). An enclosed, naturally and mechanically (via fans) ventilated stable is located centrally in the production grassland, covering an area of approximately 2.7 ha (Supplement, Fig. S1). The stable houses approximately 170 lactating cows year-round that are fed with grass silage, corn, grain, hay, and supplements. Urea and excreta are collected directly below the stable throughout the year and gives a total manure production of 5000 m^3 yr^{-1}, of which 72 % is used on-site. Another open-type stable was in operation during the second half of 2022 and has since been housing approximately 90 calves, which were originally located in the main stable.

2.2. Setup of automatic flux chambers

Three closed dynamic flux chambers (ECO_2Flux version 3.0, Dansk Miljørådgivning A/S) with an area of 0.31 m^2 and a height of 0.73 m (226.3 L total chamber volume) were used for triplicate measurements (Fig. 1). Since the area is dominated by southwestern winds (van Weerdenburg et al., 2021), the chambers were placed on the northeastern side of the stable to capture the highest atmospheric loadings emitted by the stable. The chambers were placed at a distance of 30 m facing the main stable which allowed for safe practice of the chambers away from machinery, while still being in reach of high atmospheric NH_3 concentrations that are emitted from the stable (Tulp et al., 2024). All chambers were equipped with an inner translucent chamber wall and an additional surrounding opaque chamber wall to distinguish between NH_3 fluxes during photosynthesis and respiration (Heinemeyer et al., 2013). In this paper, we only report on translucent chamber results as our aim was solely to quantify understand year round fluxes. These walls were attached in a folded position to collars that were secured in the soil for an airtight fit. At closing, the walls unfolded and lifted upwards, while the lid slowly moved downwards to ensure minimal pressure disturbances. To measure in translucent mode, only the translucent wall closed, while both the translucent and outer opaque walls closed in opaque mode. To minimize adsorption of NH_3, the translucent chamber wall and lid were constructed with fluorinated ethylene propylene (FEP) foil and the opaque wall, lid and chamber collar with PTFE-coated aluminum in order to avoid interaction with the NH_3 gas. All three chambers contained sensors that recorded PAR, chamber air temperature (°C), soil temperature (°C) (0–20 cm depth) and Soil Water Content (SWC) (%) (0–20 cm depth) each second. A small fan (spinning at 1850 rpm) was located in each chamber to avoid stratification of air inside the chamber. Air samples were pumped from the chamber (at a flow rate of 300 sccm) through a 10 m long, FEP gas tube to an ABB-LGR Ultraportable Ammonia Analyzer (UAA) located in the green equipment housing (Fig. 1) and then returned to the chamber through a second tube. The UAA measured the NH_3 concentration up to 10 ppm at a precision of 2 ppb each second through laser absorption spectroscopy. We used heated FEP gas tubes in order to avoid condensation inside the tubes. The NH_3 concentration was corrected for water vapor dilution and the effects from the absorption line broadening through the UAA directly (ABB-LGR, n.d.). Additionally, H_2O vapor was recorded up to 30,000 ppm at a precision of 50 ppm each second. Another air inlet was positioned above the equipment housing at a height of 2 m for continuous ambient concentration measurements (outside of the purging and measuring intervals, see directly below).

Fig. 1. Setup of the three automatic flux chambers with manual control boards (orange cases) attached onto the side of each chamber. At the moment of measuring, a chamber closes from the ground up after which the lid is placed on top. A small fan maintains a homogeneous trapped air column while heated FEP gas tubes collect and return air samples to the sensor and back. The equipment housing (green cart) containing the ABB-LGR Ultraportable Ammonia Analyzer and other peripherals were positioned behind the chambers (i.e. not in line with the dairy cow stable and the chambers).

The measurement schedule for an individual automated flux cycle was as follows: (i) pre-purge phase of 10 min where the ambient air was purged through the system (and measured) while the chamber was still open; (ii) flux measurement phase where the chamber was closed for a period of 5–10 min (dependent on how quickly condensation occurs); (iii) post-purge phase where, after the chamber opened again, the ambient air was pumped during 10 min and measured in order to return to atmospheric conditions inside tubes and analyzers and finally (iv) a

5 min background measurement phase where air was sampled through air inlet positioned above the sensor housing (Fig. 1). This schedule was continuously alternated between the three chambers, resulting in 48 full cycles per day. During the winter period, the number of cycles was slightly lower due to the longer (10-minute flux) measurement phase, since fluxes are low during this season (Todd et al., 2011) and prolonged measurement periods were required in order to quantify the flux. In total, 12,542 individual measurements were recorded over the whole year with 3692 flux quantifications in spring, 4075 in summer, 2241 in autumn and 2534 in winter.

A meteorological station (HOBO RX3000 Remote Monitoring Station) was installed to continuously measure meteorological data next to the automatic flux chambers (Supplement, Fig. S1). The recorded variables included PAR (μmol/(m2*sec), solar radiation (W/m2), wind direction (°), wind speed (m/s), gust speed (m/s), precipitation (mm), air temperature (°C), relative humidity (%, 'RH') and dew point (°C) at 1 min intervals. Moreover, leaf surface wetness was recorded at 1 min intervals from mid-July 2022 until the end of the measurement period using Leaf Wetness Sensors (Decagon Devices) that were placed inside each chamber.

The production grassland management practices, including cutting and fertilization with machinery, were mimicked in and around the chambers. To prevent potential biases and potential island effects from occurring around the chambers, the simulated practices were carried out at the exact same time as the management practices were done on the production grassland of the whole farm. The first slurry application was split over two days (four days apart) and hence we mimicked this application when the farmer applied slurry to the respective field where the chambers were located. The farmer applied manure through slurry injection: small gullies of approximately 3 cm wide and approximately 2 cm deep at 18 cm intervals between gullies were made in which the slurry was discharged. This was mimicked within the chamber plots by creating three gullies inside the plots; one exactly in the middle of the chamber and the two others on each side using the same dimensions as mentioned above. Slurry (produced by the cows in the main stable, Fig. S1) was retrieved directly from the slurry wagon to ensure that the same slurry composition was used. The slurry was applied in the chambers using HDPE tubes. The production grassland received 5100 m^3 slurry throughout the measurement period, equal to 51 m^3 ha^{-1}. Artificial fertilizer (AF), Calcium Ammonium Nitrate (CAN) 27 % in most cases, was distributed over the chamber plots by hand. Cutting was performed at the same height as the production grassland by manual mowing. The freshly cut grass on the agricultural field was generally removed one or two days post mowing, which was again mimicked manually within the chamber plots. We did not consider utilizing one or more of the chambers to quantify fluxes without these management practices, since an island effect of, e.g., unfertilized soils in the middle of the field would occur. This would have yielded unrealistic fluxes of unmanaged conditions.

Slurry samples were taken in triplicates directly from the slurry wagon for chemical analyses. These were then freeze-dried, milled by hand using a mortar and pestle and finally analyzed for N and C content using an elemental analyzer (Vario EL cube, Elementar GmbH, Langenselbold, Germany). N and C content (%) were determined for samples from all four slurry applications, however, the dry matter content of the last three applications could not be determined due to technical errors. In order to still estimate the amount of N and C of the slurry's wet weight for these applications, we used dry matter content of the first application,.

2.3. Setup of transect measurements on production grassland

During periods without active management practices (slurry and AF application, and cutting) and a dominant wind coming from the southwest, the spatial variability of NH_3 fluxes was assessed using a manual flux chamber. This chamber was constructed using similar building materials and chamber diameter (Supplement, Fig. S2), i.e. the chamber covered an area of 0.31 cm^2 and had a height of 0.4 m (124 L). Three installed sensors recorded PAR, chamber air temperature (°C) and relative humidity (%), respectively. During measurements, air was pumped from the chamber through a 3 m FEP heated tube to the UAA and then returned to the chamber (closed mode). Background level measurements of NH_3 with the chamber open to the atmosphere were also performed (open mode).

The measurements were conducted along two transects, one along the prevailing wind direction (NE-transect) and the other in the opposite direction (SW-transect) (Supplement, Fig. S3). Blank measurements using a PTFE-coated plate that sealed off the chamber were routinely performed as a quality control procedure. As expected, these measurements yielded a net zero flux (see Section 2.4). Hereafter, measurements were conducted in triplicates at six different distances to the stable up to a radius of 500 m (15, 31, 62.5, 125, 250 and 500 m). In order to minimize the effect of the meteorological variability a transect was measured within a three-hour window by setting the measurement and purging time both to 5 min. These timings were selected because ambient NH_3 concentrations did not show considerable variation across the transects at this temporal scale.

2.4. Flux calculation

Fluxes were derived from closed flux chamber measurements by determining the rate of concentration change in the chamber headspace over time during chamber closure (Stolk et al., 2009). Whether this rate of change in concentration should be approached linearly or nonlinearly has been extensively debated (Kutzbach et al., 2007; Stolk et al., 2009; Parkin et al., 2012; Kandel et al., 2016). The concentration gradient is altered over time due to the closed off atmosphere inside the chamber and in turn affects the course of the concentration change over time (Stolk et al., 2009; Parkin et al., 2012; Kandel et al., 2016). Approaching the flux calculation with a linear model (LM) could then cause an underestimation due to saturation in the chamber headspace creating an equilibrium state in the movement of NH_3 between the atmosphere and the landscape. However, cases where a linear model is actually considered more robust compared to a non-linear model include low flux cases and measurements where the measured curve deviates from the theoretical non-linear curve (Parkin et al., 2012; Hüppi et al., 2018). Consequently, a hybrid approach was selected where fluxes were calculated using linear regression (LM) as well as the modified Hutchinson-Mosier non-linear model (Pedersen et al., 2010). This was incorporated in a R script that included the linear flux calculation and the HMR package (R version 2023.06.0, R Core Team, 2024). The non-linear model (HMR) was selected for flux calculation when: (i) the RMSE of the HMR flux was lower than the RMSE of LM-flux and (ii) the ratio between the HMR flux and the LM flux had a maximum value of 4 (Görres et al., 2015).

In addition, any potential disturbances at the start of the measurement caused by chamber closure (i.e. the so-called 'deadband') were excluded from the calculation (see also Görres et al., 2015). For LM fluxes it is also important to exclude concentration measurements nearing the equilibrium point (referred to as 'end-time' from here on), as this ensures a more appropriate model fit. The R script included the selection of the best deadband and end time by fitting LMs at varying starting times, taking into account also the travel time from the chamber headspace to the UAA. Consequently, LMs were fitted at varying start- and end-times. The deadband and end-time were chosen based on the highest R of the fitted LMs (i.e. the best fitting model). The following constraints were incorporated in this selection procedure: (i) a minimum calculation window of 30 s (to ensure ample data availability for correct model fit) and (ii) the end-time could not exceed 90 % humidity (mean of a 60 s period) in order to avoid gaseous NH_3 losses as a result of condensation. For the non-linear approach, HMR was fitted on one calculation window based on the best deadband that was found in the

before mentioned procedure, as well as the maximum end-time determined with criterium ii.

2.5. Statistical analyses

Analyses were performed using R-software (version 4.4.2, R Core Team, 2024). The non-parametric Wilcoxon signed-rank test was performed to determine whether the management practices significantly affected fluxes. Two-week budgets were used for this, as it has previously been reported that most of the NH_3-loss following these types of practices occurred within two weeks (Mosquera et al., 2001; Spirig et al., 2010; Forrestal et al., 2016; Weber et al., 2018). Budgets for specific time periods were calculated by averaging all measured fluxes within that period and then scaling the average to the total time of the period. Furthermore, since AF was applied shortly after cutting and fluxes associated with CAN application appear to be low compared to other types of fertilizers (Forrestal et al., 2016), including slurry application, it is difficult to separate the effect of AF from the effect of cutting. Therefore, budgets were calculated from the moment of cutting until two weeks *after the following AF application*. The same resulting time period was used to compare with the pre-cutting period. Budgets were also calculated on a monthly basis to assess the seasonality of net NH_3-N fluxes with and without two-week periods following management practices to separate the fluxes during management practices from the rest of the fluxes. The non-parametric Wilcoxon rank-sum test was performed to determine whether NH_3-N fluxes varied significantly across wind directions, as well with distance to the stable as a point source. This was both done for each measurement period and for all measurement periods compiled. Finally, Pearson correlation tests and a random forest analyses were performed to identify the most important variables explaining the measured NH_3 fluxes. For this, 999 replications of a 500 tree random forest model were aggregated to mean percentages of importance, using the 'ranger' package in R (Wright and Ziegler, 2017). The tested variables were the SWC, canopy moisture conditions and the meteorological variables for which we first projected net wind vectors onto the vector between the stable and the measurement locations. To explore the multivariate structure in the meteorological data, we also performed a principal component analysis (PCA) with hourly aggregates of the meteorological conditions in the hour preceding the flux measurements (i.e. air temperature, dewpoint, relative humidity, PAR, solar radiation, rain and wind projections from the stable to the flux chambers).

3. Results

3.1. Temporal variability of NH_3 fluxes

3.1.1. NH_3 fluxes after management practices

NH_3-N fluxes (in μg m^{-2} s^{-1}) (Fig. 2) showed distinct periods of elevated emission peaks following slurry application (black, broken lines), as well as more variable emission increases following other management practices (brown, dotted lines and green lines) throughout the different seasons.

Post-slurry application NH_3-N fluxes were characterized by immediate sharp emission peaks that leveled off at an exponential rate within the first 30–70 h after application (Fig. 3). During the first slurry application in March, the grassland received the largest, though most diluted, volume of slurry with an applied amount of 73.1 kg N ha^{-1} (Table 1). This application was followed by emission peaks of up to 16.8 μg NH_3-N m^{-2} s^{-1}, whereafter fluxes quickly declined, yet remained elevated during the following 65 h (Fig. 3a). After this, the fluxes dropped to a level below 0.5 NH_3-N μg m^{-2} s^{-1}. In the two-week period after the slurry application, total NH_3-loss via emission amounted to 4.1 kg NH_3-N ha^{-1}, equal to 5.7 % of the N-input of the fertilization event (Table 1). The second slurry application in the beginning of June led to the highest observed emission peak during the measurement period, when emissions reached a level of 34.3 μg NH_3-N m^{-2} s^{-1} (Fig. 3b). During this application a lower, though more concentrated, volume of slurry was applied followed by AF application. This amounted to an N input of 81.1 kg N ha^{-1} (Table 1). Fluxes decreased more rapidly in comparison to the first slurry application with 90 % of the total emitted NH_3-N being emitted during the first two days compared to five days during the first slurry application. During the two-week period after the application, a total of 3.8 kg ha^{-1} was emitted, equal to 4.7 % of the N-input through fertilization. The peak fluxes after the third slurry application at the end of June (13.5 μg m^{-2} s^{-1}) were comparable to those during the first slurry application (Fig. 3c), despite receiving less nitrogen from slurry (51.6 kg N ha^{-1}) and no additional AF. However, fluxes declined much more rapidly with 90 % of the total emitted NH_3-N being emitted after just one day. A total of 4.6 kg NH_3-N ha^{-1} was emitted during the two-week period after the application, equal to 8.9 % of the N-input of 51.5 kg ha^{-1} (Table 1). The fourth and final slurry application at the end of August was characterized by much lower fluxes in comparison to the other slurry applications with peak fluxes (up to 0.9 μg m^{-2} s^{-1}) being more than 10-fold lower (Fig. 3d). As a result, the NH_3-N loss was considerably lower with a total loss of 0.4 kg N ha^{-1}, which only represented 1.0 % of the N-input of 38.0 kg ha^{-1} (Table 1).

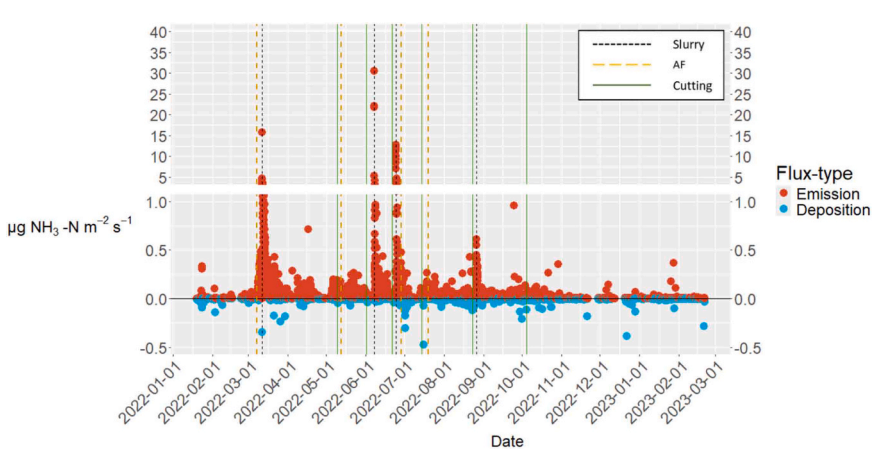

Fig. 2. Time series of NH_3-N fluxes (in μg m^{-2} s^{-1}) in the production grassland (*L. perenne*) at the dairy farm from February 2022 until February 2023. Each point represents a single chamber measurement (n = 3). Positive fluxes (i.e. net NH_3 emission) are marked in red and negative fluxes (i.e. net NH_3 deposition) are marked in blue. Black, broken lines indicate time points of slurry application, while brown, yellow broken lines and green lines indicate time points of AF application and cutting, respectively.

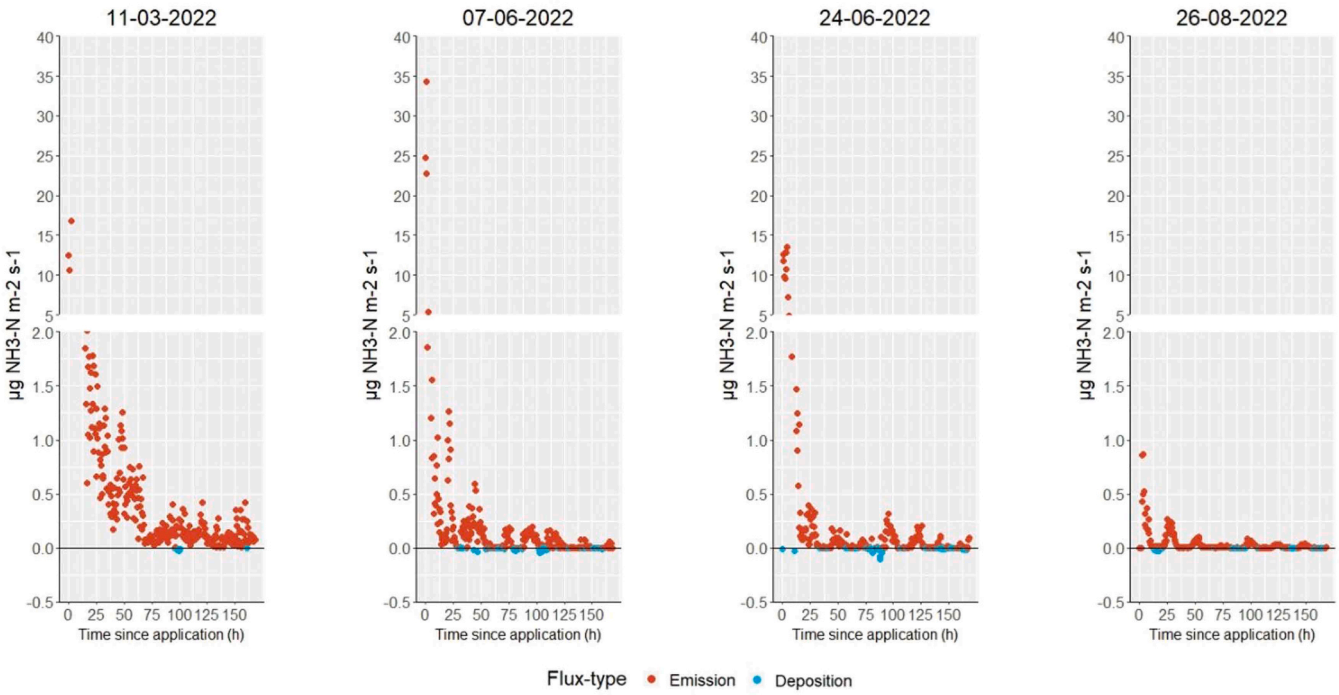

Fig. 3. Course of all measured NH_3-N fluxes in (µg m^{-2} s^{-1}) across the three automatic flux chambers during the first 150 h after slurry application at the four different application events.

During the first time that AF was applied, flux characteristics (Supplement, Table S1) followed those observed in the two-week period after the first slurry application with a total emission of 4.47 kg NH_3-N ha^{-1} and a net flux balance of 4.21 kg NH_3-N ha^{-1} due to the overlap of the periods (Supplement, Fig. S4). Flux characteristics for the third AF application were much lower with a total emission of 0.31 kg NH_3-N ha^{-1} and a net flux balance of 0.11 kg NH_3-N ha^{-1}, despite overlapping with slurry application as well (Supplement, Fig S4). Similar values were observed during the second and fourth AF application (Supplement, Table S1), which received a total of 68.0 and 27.0 kg N ha^{-1} respectively. Peak fluxes during these applications reached 0.26 µg m^{-2} s^{-1} for the second and 0.13 µg m^{-2} s^{-1} fourth application. However, no significant difference was observed between the balances before and after the second and fourth AF application in combination with cutting (Supplement, Table S2).

3.1.2. NH_3-N fluxes throughout the measurement period

The increased emissions directly following slurry application led to a monthly higher net NH_3-N emission of approximately 5.2 kg ha^{-1} and 5.7 kg ha^{-1} in March and June respectively, while a noticeably smaller peak (approximately 0.4 kg ha^{-1}) was visible in August when the last slurry application was performed (Fig. 4a). The rest of the monthly balances mostly remained below 0.3 kg NH_3-N ha^{-1}. The monthly balances reveal that 99.6 % of the net emission took place within the growing and harvesting season (March to September), while neither emission nor deposition were apparent (or at least very low) during autumn and winter. Accumulating the monthly balances yielded a net annual flux balance of 12.0 kg NH_3-N ha^{-1} y^{-1} (Supplement, Fig. S5). A similar pattern was observed for the monthly balances when excluding the two weeks post-fertilization (Fig. 4b). Interestingly, the balance in July was similar to the balances observed during autumn and winter. In contrast, the balance of August was the highest of all months with a net flux balance of over 0.2 kg NH_3-N ha^{-1} $month^{-1}$. At the annual scale, the net emissions during the four two-week periods following management practices amounted to 10.0 kg NH_3-N ha^{-1}, while the remaining ~44 weeks only amounted to 2.0 kg ha^{-1} (Supplement, Fig. S5).

When excluding the two-week period after the four slurry applications, several meteorological and other measured variables correlated significantly with the measured NH_3-N fluxes (Fig. 5). The strongest observed relationships were a positive effect of solar radiation (Fig. 5b; $R = 0.43$, $p < 0.01$) and a negative effect of relative humidity (Fig. 5d; $R = -0.44$, $p < 0.01$). Both air and soil temperature were positively, but relatively weakly, correlated with NH_3-N fluxes with $R = 0.29$ and 0.21 ($p < 0.01$) respectively (Figs. 5a and 5f). The results for the other measured environmental variables showed weak ($R < 0.2$, $p < 0.01$) or no relationship (wind projection) with NH_3-N fluxes. It is also noteworthy that as soon as precipitation and leaf wetness increased, fluxes were near-zero (Fig. 5c and Fig. 5h, respectively). The same is true when wind originated from the SSE direction, while the largest variability in fluxes were observed when the wind originated from SEE or S direction (see Supplement Fig. S6). Interestingly, when the four two-week periods after slurry application events were included in these analyses, the directions of all the observed correlations remained the same, albeit with much weaker relationships ($R = -0.19$ for leaf wetness, $p < 0.01$ and $R < 0.10$ for all other cases, Supplement, Fig. S7). This is likely due to the strong positive fluxes observed during the fertilization event (see Section 3.1.1, Supplement Fig. S8). In addition to these independent correlations between the NH_3 fluxes and the measured variables, random forest analysis for all fluxes (excluding those up to two weeks after manure application) identified the following order of top predictors for ammonia fluxes (see Supplement Table S3a): Photosynthetically active radiation (normalized mean 24.40 %, standard deviation 2.43 %), air temperature (normalized mean 23.02 %, standard deviation 2.21 %), dewpoint (normalized mean 21.24 %, standard deviation 1.31 %), solar radiation (normalized mean 17.27 %, standard deviation 2.20 %), relative humidity (normalized mean 13.21 %, standard deviation 1.04 %), wind projection (normalized mean 0.82 %, standard deviation 0.09 %), and rain (normalized mean 0.05 %, standard deviation 0.01 %). General model fit, quantified as the out-of-bag R^2, was moderate with 36.0 % variance explained by meteorological variables, meaning that fluxes were influenced for a large part by other factors than meteorology. When running random forest analyses on only the fluxes during, and two weeks after, farming practices, the order of top predictors shifted: temperature, relative humidity, dewpoint,

Table 1
Summary of slurry amount and quality, NH_3-N fluxes and meteorological variables calculated over the two-week periods after each slurry application during 2022. Values are given as absolute values or means ± SE. N.A. refers to no additional CAN application.

Slurry application	Unit	1st	2nd	3rd	4th
Date	dd-mm-yy	11–03–22	07–06–22	24–06–22	26–08–22
Cattle slurry	m^3 ha^{-1} ww*	40	20	20	20
Ditch water	m^3 ha^{-1}	5	5	5	0
C	%	34.78 ± 0.37	39.16 ± 0.25	36.24 ± 0.39	42.33 ± 0.10
N	%	2.59 ± 0.09	2.16 ± 0.09	3.29 ± 0.06	3.03 ± 0.03
C/N		13.43 ± 0.31	18.16 ± 0.70	11.02 ± 0.11	13.96 ± 0.14
N-content in slurry dry matter	kg ha^{-1}	73.13 ± 2.46	33.84 ± 1.41	51.54 ± 0.94	37.98 ± 0.38
Additional CAN 27 %	kg ha^{-1}	N.A.	175	N.A.	N.A.
Maximum NH_3-N flux	µg m^{-2} s^{-1}	16.79 ± 0.01	34.27 ± 0.26	13.51 ± 0.08	0.87 ± 0.02
Net NH_3-N balance	kg ha^{-1}	3.85 ± 0.07	2.56 ± 0.05	3.01 ± 0.05	0.28 ± 0.03
NH_3-N loss	kg ha^{-1}	4.13 ± 0.07	3.81 ± 0.07	4.61 ± 0.06	0.37 ± 0.03
NH_3-N loss / N-input	%	5.7	4.7	8.9	1.0
Time until 90 % loss of NH_3-N	h	132	43	22	247
Mean air temperature	°C	8.3	15.8	17.4	18.6
Total precipitation	mm	4.4	10.4	32.2	31.0
Mean RH	%	80.5	81.3	81.0	73.4
Mean SWC during application	%	38.2	31.3	20.9	9.4

* 'ww' = 'wet weight'.

photosynthetically active radiation, solar radiation, followed by near zero attributes of rain and wind projection (with normalized means of 38.10, 23.09, 16.79, 11.69, 10.86, 0.01, and −0.54; and standard deviations of 6.59 2.92 2.90 1.84 1.56 0.01 0.26, respectively; see Supplement Table S3b); for this random analyses, average out-of-bag R^2 was lower (8.9 %).

The PCA revealed that the first principal component ('PC1') accounted for 44.3 % of the total variance and described a gradient from warm, sunny and relatively dry to colder, low radiation, humid conditions, with positive loadings for temperature, dewpoint, PAR and solar radiation and a negative loading for RH (see Supplement Fig. S9), coinciding with environmental variables that predict ammonia fluxes from the random forest analysis. The second component ('PC2') explained 19.8 % of the total variance and mainly varied over radiation conditions (with positive loadings for dew point, temperature, RH and rain and negative loadings for PAR, solar radiation and wind originating from the stable, Supplement Fig. S9). Together, PC1 and PC2 captured 64.2 % of the variance in meteorological variables, confirming that that solar radiation & PAR and temperature & dew point were strongly collinear and were largely captured by these two axes of variation.

3.2. Spatial variability in NH_3 fluxes

Three transects were performed in July, September and October (Fig. 6). The NE-transect in July revealed high variability near the stable (within 70 m distance) with fluxes ranging between −0.04 and 0.06 µg m^{-2} s^{-1}, but generally depicting emission (Fig. 6a). As the distance from the stable increased, the variability decreased with fluxes stabilizing at near-zero values. In contrast, the SW transect in July was dominated by negative NH_3 fluxes, i.e. deposition, with the exception of the first sampling points (up to 31 m distance). Fluxes started out high and dropped slightly below zero at distances of 61.5–125 m, after which a further decrease in fluxes was observed at 250 m before fluxes slightly increased again at a distance of 500 m. As a result, we found a negative relation between NH_3 fluxes at the SW transect and distance from the stable ($R = -0.51$, $p < 0.01$), while no significant relationship was found at the NE transect ($p > 0.05$). The transects conducted in September and October showed different patterns as stable deposition rates were observed across the whole NE transect in September, while the SW transect showed a shift from deposition towards emission at some point between 125 and 250 m distance from the stable. This again

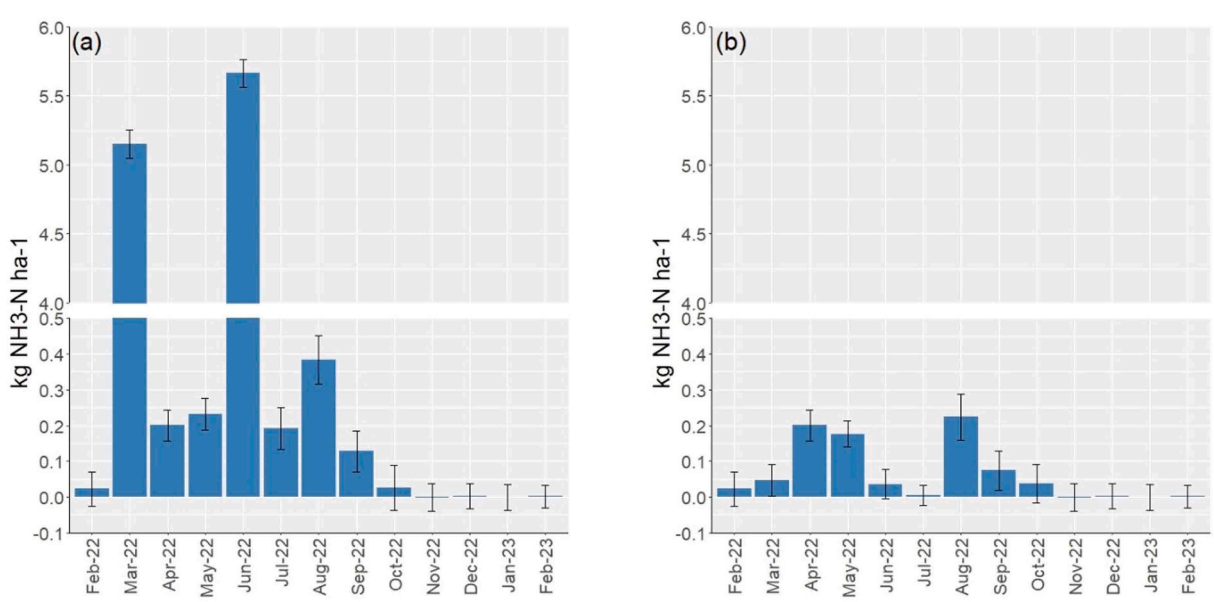

Fig. 4. Average monthly net flux balance (in kg NH_3-N ha^{-1}, n = 3, ± SE) from February 2022 until February 2023; (a) including the periods after management practices with slurry applications in March, twice in June and in August and (b) excluding two-week periods after management practices.

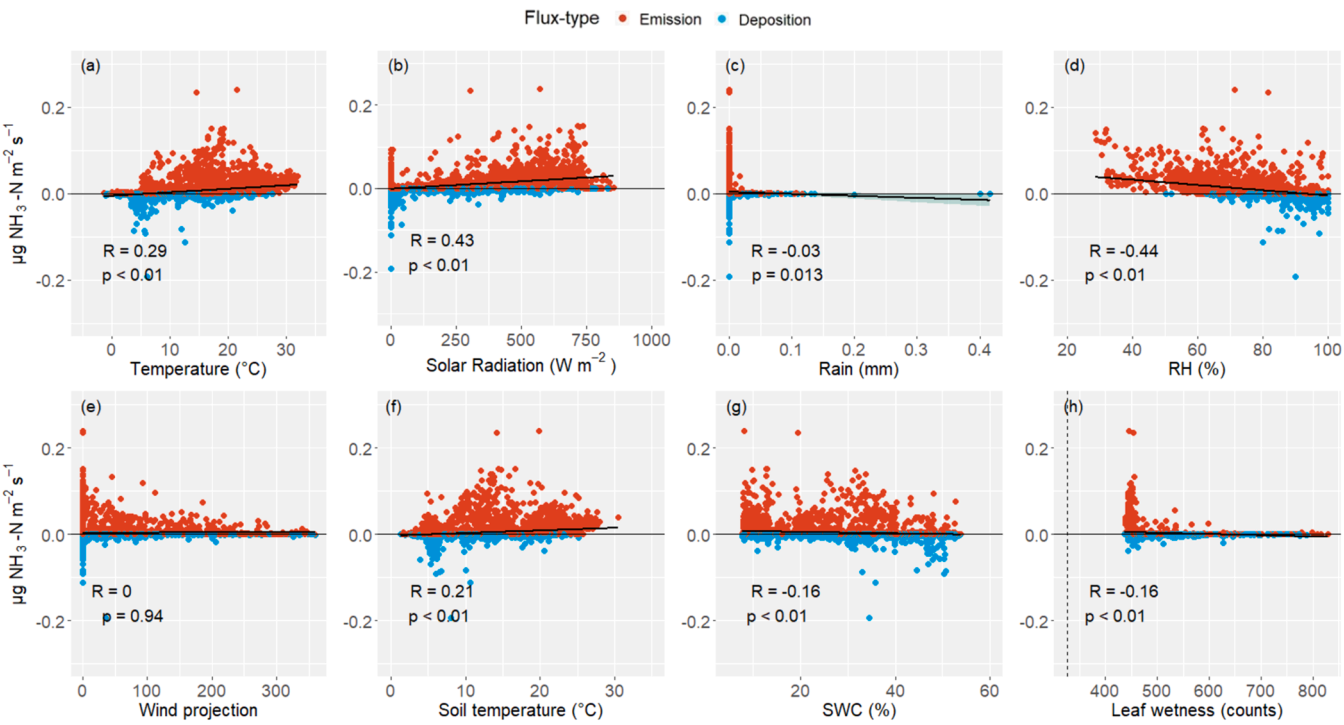

Fig. 5. Pearson correlation between NH_3-N fluxes (in µg m^{-2} s^{-1}, excluding the two weeks post slurry application events) and air temperature (a, 1 h average), solar radiation (b, 1 h average), precipitation (c, 1 h average), relative humidity (d), wind projection (e, from the dairy stable), soil temperature (f, 1 h average), Soil Water Content (g) and leaf wetness (h) with corresponding coefficients and *p*-values.

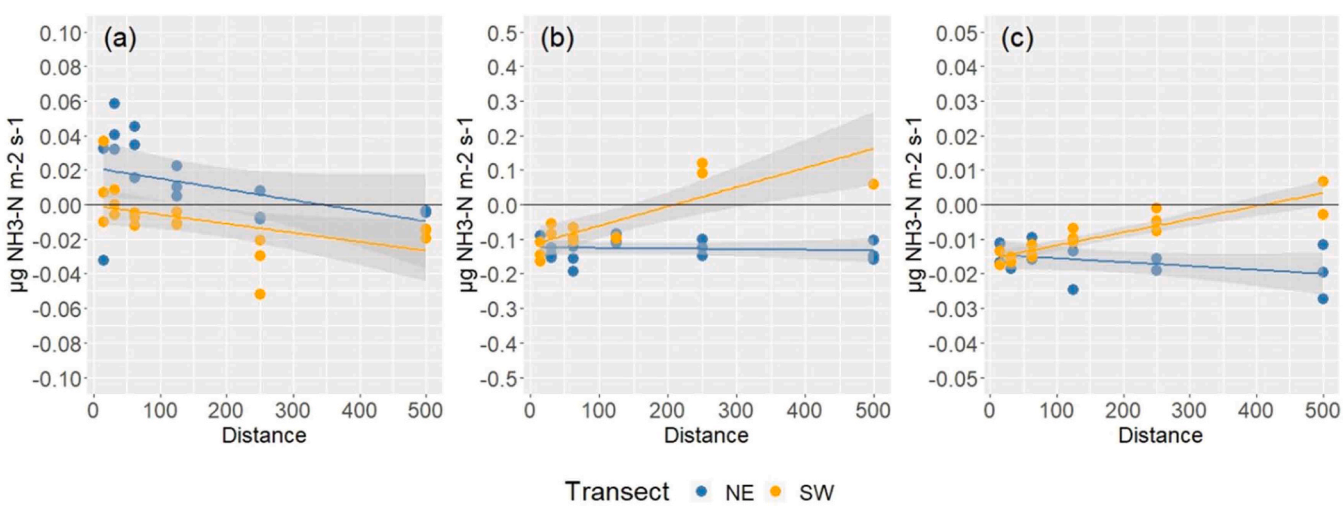

Fig. 6. NH_3 fluxes (in µg NH_3-N m^{-2} s^{-1}) along the NE- and SW-transects with increasing distance from the stable for July (a), September (b) and October (c). Note that the y-axis range varies for each plot. Note that the amount of vegetation at the SW transect was considerably lower than at the NE transect during the first measurement (July), since the fields in the SW were levelled early Spring and resown with *L. perenne*.

revealed a significant, though now positive, relationship (R = 0.79, $p < 0.01$) between NH_3 fluxes at the SW transect and distance from the stable, but none at the NE-transect. A similar pattern was observed in October, though fluxes along the NE-transect showed a small decrease. The October measurements revealed a correlation coefficient of 0.91 ($p < 0.01$) between NH_3 fluxes at the SW transect and distance from the stable and no significant relationship at the NE transect. In addition, results from the non-parametric Wilcoxon rank-sum test showed that the fluxes found at the SW-transect were significantly different from those along the NE-transect for each month ($p < 0.05$). When the fluxes from the different months were compiled, no significant difference was found between the fluxes at the NE-transect and those at the SW-transect. Despite this, a weaker relationship could still be identified between the distance from the stable and the compiled fluxes at the SW-transect (R = 0.34, $p < 0.05$). No significant relationship was found for the compiled fluxes along the NE-transect.

4. Discussion

4.1. Net annual fluxes

We found a detailed temporal pattern of NH_3 fluxes over a full year of intensive flux chamber measurements with profound positive net fluxes, i.e. NH_3 emissions, particularly during the growing and harvesting

season between March and September. This is also evident since most of the NH_3-loss via emission occurred during this timeframe with net monthly NH_3 balances varying between 0.1 and 5.6 kg NH_3-N ha^{-1}. Slurry applications were associated with sharp peaks during the day time in NH_3 fluxes lasting between 30 and 70 h. These post-slurry fluxes comprised the majority of the NH_3 loss as revealed by the large difference in net balance between the first two weeks after the slurry application and the remaining 44 weeks: 10 kg NH_3-N ha^{-1} yr^{-1} vs 2 kg NH_3-N ha^{-1} respectively (Fig. 4). This indicates also the relevance of intensive temporal monitoring to comprise the total ammonia emission budget. In contrast, the data collected during fall and winter suggest that neither deposition nor emission are prominent with near-zero net monthly balances not exceeding 0.02 kg NH_3-N ha^{-1}. This is likely explained by the reduced overall biological activity of both soil microbes and plants involved in the production of NH_3 as their activity is highly temperature dependent. Additionally, the environmental conditions during autumn and winter (wet surface area and reduced air temperatures) are keeping relatively more NH_3 dissolved. Overall, the measured fluxes yielded a net annual emission of 12 kg ha^{-1}; a net source of NH_3-N. With a total N-input of 402 ± 5 kg ha^{-1} through slurry application and artificial fertilizers, this amounts to a fractional NH_3-N atmospheric emission loss of approximately 3 %. This fraction of total N-input on our specific test field is relatively large, but equals the regulatory limit based on the total application surface of the farmers.

Similar seasonal patterns were observed in other studies (e.g. Mosquera et al., 2001; Todd et al., 2011; Van Damme et al., 2015). Mosquera et al. (2001) reported that higher emission rates were generally observed during summertime resulting in net monthly fluxes ranging between 1.0 and 5.5 kg ha^{-1} during the growing and harvesting season at their study site in the Netherlands. At the same time, lower emission and deposition rates were observed during wintertime, yielding net monthly fluxes ranging between −0.3 and 0.5 kg ha^{-1}. Still, the intensively managed grassland in their study yielded an accumulated emission of approximately 26 NH_3 kg ha^{-1} for a 25-month period. This averages to 12-month net annual emission of 10.3 NH_3-N kg ha^{-1} and a fractional loss of approximately 4 %, which closely resembles what was found in the present study. This is interesting, as Mosquera et al. (2001) used tower-based instruments in their setup, which means this value represents part of the flux that is determined by aerodynamic transport as a result of meteorological conditions and atmospheric turbulence strength as well (Sutton et al., 1998a; Zhang et al., 2021). Using similar tower-based techniques, Flechard et al. (2010) reported a net annual emission of 17 NH_3-N kg ha^{-1} at their study site in the Swiss Alps, which represented approximately 11 % of the N-input over four slurry application events. Differences in the amplitude of reported net annual fluxes may partly be a result of different measuring techniques, but we expect that these differences can be attributed more strongly to varying management strategies, livestock density, climate, soil conditions and grassland composition (Flechard et al., 2010). Though these conditions vary across these study sites and different measuring methods were used, the findings clearly demonstrate that the major part of NH_3 loss is driven by the application of slurry, emphasizing that grasslands are net sources of NH_3 due to animal husbandry and fertilization events (David et al., 2009; Flechard et al., 2013).

4.2. Effect of management practices

NH_3 fluxes directly after slurry application increase sharply during day time and vary in both magnitude and duration. Such sharp flux increases are common after fertilization because the slurry injection, while meant to reduce ammonia emissions, still leaves slurry exposed to the atmosphere, leading to direct exchange of ammonia with the atmosphere via volatilization (Duncan et al., 2017). Peak fluxes varied between 13.5 and 34.3 μg m^{-2} s^{-1} during the first three slurry applications, while the last slurry application resulted in a notably lower peak of 0.9 μg m^{-2} s^{-1}. In all cases, it is apparent that after the sharp increase in fluxes directly after slurry application, the fluxes exponentially decrease back to background fluxes (Fig. 3). This pattern has been observed in other studies as well (Van der Molen et al., 1990; Spirig et al., 2010). However, the duration of these enhanced post-slurry fluxes varies with 90 % of NH_3-N being volatilized within 48 h during the second and third slurry application, while this took 132 and 247 h for the first and last slurry application, respectively. The variation in extent and duration of enhanced post-slurry fluxes may be explained by the amount and quality of the slurry, as well as by varying environmental conditions. This is shown in literature where peaks of up to 47 μg m^{-2} s^{-1} (Thompson and Meisinger, 2005), 56 μg m^{-2} s^{-1} (Rumburg et al., 2006) and even 70 μg m^{-2} s^{-1} (Spirig et al., 2010; Flechard et al., 2010) have been reported. Spirig et al. (2010) state that the size of the field to be fertilized is an important determinant of NH_3 volatilization, as this affects the saturation in the air column and thus the exchange of NH_3 between the surface and atmosphere. Their study site was over 20-fold smaller than the fertilized area in the present study, resulting in a larger surface-air concentration difference than what would be the case for the 100-ha production grassland in this study. This likely explains much of the at least twofold difference in peak flux compared to the present study. Despite receiving the largest slurry volume during the first application, the peak flux and the rate at which the resulting enhanced flux decreased were much smaller compared to the following slurry application (Fig. 3a). Moreover, the amount of NH_3-N that was lost during the two-week period following the application represented 5.7 % of the N-content in the slurry dry matter. However, SWC was highest during this first application and the southern plots of the production grassland were already fertilized with cattle slurry four days prior to the application at the experimental site, which already elevated the ambient air concentrations. Both may have inhibited NH_3-loss due to faster infiltration into the soil and due to lower surface-air concentration differences (Flechard et al., 2010). In contrast, the fast emission and large peak fluxes during the second and third slurry application may be the result of the drier conditions during the summer. These dry conditions were even more prominent at the end of summer in August, however, the post-slurry fluxes during the application in August did not follow a similar course. Instead, the peak flux was 10-fold lower than those during the other slurry applications, while the emission of NH_3 occurred at a more gradual rate. It should be noted that the slurry was not diluted during this application, giving it a relatively high dry matter content compared to the other applications. This should also promote further NH_3 loss to the atmosphere (Flechard et al., 2010), yet this was not observed. One explanation for the relatively low NH_3-loss after the August slurry application could be that relatively high emissions were already observed apart from the two-week periods following management practices leading to a lower surface-air concentration difference, thereby inhibiting rapid NH_3 emission.

4.3. Combination of cutting and artificial fertilizer application

We found no significant effects on both NH_3 fluxes and balances after the combined practice of AF application and cutting. Previous studies showed that NH_3 loss from CAN can be between < 1 % and 4 % of applied N (Black et al., 1985; van der Weerden and Jarvis, 1997; Forrestal et al., 2016), where higher losses are likely attributed to more rapid dissolution of $CaCO_3$ in CAN. Since the environmental conditions during and after the second and fourth AF application in the present study were relatively dry, this has likely contributed to a slow dissolution of CAN and thus a slower and more gradual release of NH_3, potentially resulting in less prominent peaks that were indistinguishable from background levels. Since all AF applications were done in combination with cutting, it is worth considering how this practice may have affected net post-application fluxes. Cutting was only performed once without subsequent fertilization at the end of the growing and harvesting season, but this also did not show distinct increases or decreases in NH_3 fluxes. Weber et al. (2018) observed NH_3 losses after cutting and

litter removal with peaks occurring after three to nine days. In contrast, David et al. (2009) reported that the emissions observed after cutting predominantly originated from litter and that the cut plants did not act as a significant NH_3 source. Weber et al. (2018) also argued that the re-growth of the plant after it has been cut increases ammonium levels in the leaf tissue (i.e. apoplastic ammonium), which in turn enhances NH_3 emissions. Other mechanisms that may lead to an increase in emissions include the prevention of recapture of below canopy emissions, damage to the leaves as a result of the cut, or a reduction in substrate N consumption into structural N in the plant (Massad et al., 2010). Our hypothesis for not observing enhanced NH_3 emissions after cutting is that the air column was already relatively saturated with NH_3 (given the observed relatively high levels), which reduces the surface-air concentration difference and thus restricting the movement of NH_3 towards the atmosphere (Flechard et al., 2010). This indicates that local level flux dynamics are at play depending on the distance to the point source of NH_3 (i.e. the stable), which should be taken into account for flux quantification of entire production grasslands.

4.4. Spatial patterns

We found distinct variability in NH_3 fluxes depending on the distance to the stable as well as wind direction. Not only did the fluxes vary spatially, these spatial patterns also varied over time. Earlier in the season, we found that irrespective of wind direction emissions of NH_3 occurred close to the stable while deposition occurred further away. However, later in the season and depending on wind direction, we actually observed deposition close to the stable and emission further away.

In another study performed at the same farm, the spatial variation in ambient atmospheric NH_3 concentrations was assessed (Tulp et al., in prep). The highest NH_3 concentrations were observed directly next to the ventilation grills of the stable on the NE side and were up to a threefold higher (up to 800 NH_3 μg m^{-3}) than the concentrations found at the NW, SW and SE side. In all directions, the concentration quickly declined to < 100 NH_3 μg m^{-3} within 100 m (at a height of 1.5 m) and to indistinguishable from background concentration levels within 500 m. Assuming equal soil and vegetation conditions across the complete 500 m transects, increasing fluxes would be expected when ambient NH_3 concentrations decline due to increased surface-air concentration differences (Flechard et al., 2010). This would be visible through an increase in emissions, a decrease in deposition rates or even an increase in bidirectional fluxes, meaning that fluxes may start shifting from deposition to emission (Sutton et al., 1998b). However, soil and vegetation conditions likely also vary and the measured fluxes reveal a different pattern, suggesting that these conditions play a crucial role in the exchange of NH_3. Again, this can be explained by the surface-air concentration difference, which is a product of both the atmospheric concentration and the nitrogen status of the landscape. This determines the direction and strength of the movement of NH_3. Taking this into consideration, and in addition to the previously mentioned local flux dynamics, continuous measurements at a larger distance from the stable (where atmospheric concentrations are lower) could potentially have revealed a different course of NH_3 fluxes throughout the one-year period. For such measurements, our method of using automated and manual flux chambers to measure ammonia emission and deposition yielded high frequency data at a small scale, making this a viable strategy to study such local dynamics. Such a type of study should further be complemented by investigating individual processes, such as mechanisms that affect NH_3 exchange of the external leaf area, as present flux models are lacking proper parametrization (Jongenelen et al., 2025).

The observed monthly variation in NH_3 emissions indicate that seasonal variation plays an important role in the spatial flux patterns as well. Nevertheless, the vast majority of net NH_3 emissions was evidently caused by slurry application. During these events, the surface-air concentration difference is likely to be near-equal across the grassland. This is due to homogenous slurry application with a concentration far greater than the ambient air concentration prior to slurry application, resulting in a near-homogenous NH_3 emission flux across the production grassland. Although spatial variation exists in background fluxes and would therefore affect the net annual NH_3 balance, this represents a small fraction of post-slurry fluxes and this variation would likely have a minimal effect on these types of fluxes. One can therefore assume a uniform net annual NH_3-N emission of 12 kg ha^{-1} across this production grassland.

5. Conclusion

This study shows that slurry application induces significant levels of NH_3 emission from temperate production grassland, which is important for sink-source dynamics at dairy farms during the growing and harvesting season. The NH_3 fluxes varied spatially and temporally across the production grassland and background fluxes outside of specific post-slurry application periods only represented a small fraction of total fluxes. We found a net annual emission of 12 NH_3-N kg ha^{-1} across the production grassland with a fractional NH_3 loss of 3 %. This makes the dairy farm production grassland a net NH_3 source in terms of atmospheric exchange. Most of the NH_3 emission was clearly driven by the slurry applications, but the amplitude in emissions was determined by environmental conditions, especially with enhanced emissions during warm and dry conditions. Although this only a first step into researching the small scale dynamics of atmosphere-biosphere fluxes of ammonia, our chamber techniques proved valuable to investigate such NH_3 fluxes and variables that influence these fluxes. Presently, the Dutch dairy sector faces a large task to comply with proposed NH_3 reductions in accordance to international policies. This research, although only performed at one farm for one year in a temperate climate, implies that applying slurry dependent on local weather conditions can vastly limit gaseous emission which aids in reducing NH_3 losses that benefit both farmer and the natural environment.

CRediT authorship contribution statement

Roland Bol: Writing – review & editing. **Bram Ebben:** Writing – review & editing, Methodology, Investigation. **Tamar Tulp:** Writing – review & editing, Visualization, Formal analysis, Data curation. **Klaus S. Larsen:** Writing – review & editing, Methodology. **Barmentlo S. Henrik:** Writing – review & editing, Writing – original draft, Supervision, Methodology, Funding acquisition, Formal analysis, Conceptualization. **Emiel E. van Loon:** Writing – review & editing, Writing – original draft, Funding acquisition, Formal analysis, Conceptualization. **Albert Tietema:** Writing – review & editing, Writing – original draft, Supervision, Funding acquisition, Conceptualization. **Claudia C. Schwennen:** Writing – review & editing, Writing – original draft, Visualization, Methodology, Investigation, Formal analysis, Data curation, Conceptualization.

Declaration of Competing Interest

The authors declare no conflict of interest.

Acknowledgements

This project was funded by the foundation Mesdag-Zuivelfonds NLTO. We are grateful to the farmers for their hospitality and for their help with the experiments. We also thank Jasmijn van Gool, Chloë Roberts, Willona Ortsen and Tristan Jansen and staff of the IBED-UvA laboratory for helping with the experiments and/or analyses.We also thank the developers of the ECO_2Flux (version 3.0) flux chambers at Dansk Miljørådgivning A/S for their close collaboration on the development of the chambers. Finally, we thank two anonymous reviewers

for their valuable suggestions that strengthened this paper.

Appendix A. Supporting information

Supplementary data associated with this article can be found in the online version at doi:10.1016/j.agee.2026.110258.

Data availability

We will upload all data into a public repository upon publication

References

2023. Central Statistics Office (CBS), Grasland; oppervlakte en opbrengst. https://www.cbs.nl/nl-nl/cijfers/detail/7140gras.

ABB-LGR (n.d.). Ultraportable Ammonia Analyzer Datasheet.⟨https://www.et.co.uk/assets/resources/datasheets/LGR%20Portable%20Ammonia%20Analyzer%20Product%20Datasheet.pdf⟩.

Black, A.S., Sherlock, R.R., Smith, N.P., Cameron, K.C., Goh, K.M., 1985. Effects of form of nitrogen, season, and urea application rate on ammonia volatilisation from pastures. New. Zeal. J. Agr. Res. 28, 469–474. https://doi.org/10.1080/00288233.1985.10417992.

David, M., Loubet, B., Cellier, P., Mattsson, M., Schjoerring, J.K., Nemitz, E., Sutton, M. A., 2009. Ammonia sources and sinks in an intensively managed grassland canopy. Biogeosciences 6 (9), 1903–1915. https://doi.org/10.5194/bg-6-1903-2009.

Delon, C., Galy-Lacaux, C., Serça, D., Loubet, B., Camara, N., Gardrat, E., Mougin, E., 2017. Soil and vegetation-atmosphere exchange of NO, NH_3, and N_2O from field measurements in a semi-arid grazed ecosystem in Senegal. Atmos. Environ. 156, 36–51. https://doi.org/10.1016/j.atmosenv.2017.02.024.

Duncan, E.W., Dell, C.J., Kleinman, P.J.A., Beegle, D.B., 2017. Nitrous oxide and ammonia emissions from injected and broadcast-applied dairy slurry. J. Environ. Qual. 46 (1), 36–44. https://doi.org/10.2134/jeq2016.05.0171.

Einarsson, R., Cederberg, C., Kallus, J., 2018. Nitrogen flows on organic and conventional dairy farms: a comparison of three indicators. Nutr. Cycl. Agroecosyst. 110, 25–38. https://doi.org/10.1007/s10705-017-9861-y.

Fang, F., Han, X., Liu, W., Tang, M., 2020. Carbon dioxide fluxes in a farmland ecosystem of the southern Chinese Loess Plateau measured using a chamber-based method. PeerJ 8, e8994. https://doi.org/10.7717/peerj.8994.

Feest, A., van Swaay, C., van Hinsberg, A., 2014. Nitrogen deposition and the reduction of butterfly biodiversity quality in the Netherlands. Ecol. Ind. 39, 115–119. https://doi.org/10.1016/j.ecolind.2013.12.008.

Flechard, C.R., Massad, R.S., Loubet, B., Personne, E., Simpson, D., Bash, J.O., Sutton, M. A., 2013. Advances in understanding, models and parameterizations of biosphere-atmosphere ammonia exchange. Biogeosciences 10 (7), 5183–5225. https://doi.org/10.5194/bg-10-5183-2013.

Flechard, C.R., Spirig, C., Neftel, A., Ammann, C., 2010. The annual ammonia budget of fertilised cut grassland–Part 2: seasonal variations and compensation point modeling. Biogeosciences 7 (2), 537–556. https://doi.org/10.5194/bg-7-537-2010.

Forrestal, P.J., Harty, M., Carolan, R., Lanigan, G.J., Watson, C.J., Laughlin, R.J., Richards, K.G., 2016. Ammonia emissions from urea, stabilized urea and calcium ammonium nitrate: insights into loss abatement in temperate grassland. Soil Use Manag 32, 92–100. https://doi.org/10.1111/sum.12232.

Görres, C.M., Kammann, C., Ceulemans, R., 2015. Automation of soil flux chamber measurements: potentials and pitfalls. Biogeosci. Discuss. 12(17. https://doi.org/10.5194/bg-13-1949-2016.

Heinemeyer, A., Gornall, J., Baxter, R., Huntley, B., Ineson, P., 2013. Evaluating the carbon balance estimate from an automated ground-level flux chamber system in artificial grass mesocosms. Ecol. Evol. 3 (15), 4998–5010. https://doi.org/10.1002/ece3.879.

Hoffmann, M., Jurisch, N., Garcia Alba, J., Albiac Borraz, E., Schmidt, M., Huth, V., Augustin, J., 2017. Detecting small-scale spatial heterogeneity and temporal dynamics of soil organic carbon (SOC) stocks: a comparison between automatic chamber-derived C budgets and repeated soil inventories. Biogeosciences 14 (4), 1003–1019. https://doi.org/10.5194/bg-14-1003-2017.

Hüppi, R., Felber, R., Krauss, M., Six, J., Leifeld, J., Fuß, R., 2018. Restricting the nonlinearity parameter in soil greenhouse gas flux calculation for more reliable flux estimates. PLoS ONE 13 (7), e0200876. https://doi.org/10.1371/journal.pone.0200876.

Jongenelen, T., Van Zanten, M., Dammers, E., Wichink Kruit, R., Hensen, A., Geers, L., Erisman, J.W., 2025. Validation and uncertainty quantification of three state-of-the-art ammonia surface exchange schemes using NH3 flux measurements in a dune ecosystem. Atmos. Chem. Phys. 25 (9), 4943–4963. https://doi.org/10.5194/acp-25-4943-2025.

Kandel, T.P., Lærke, P.E., Elsgaard, L., 2016. Effect of chamber enclosure time on soil respiration flux: A comparison of linear and non-linear flux calculation methods. Atmos. Environ. 141, 245–254. https://doi.org/10.1016/j.atmosenv.2016.06.062.

Kutzbach, L., Schneider, J., Sachs, T., Giebels, M., Nykänen, H., Shurpali, N.J., Wilmking, M., 2007. CO_2 flux determination by closed-chamber methods can be seriously biased by inappropriate application of linear regression. Biogeosciences 4 (6), 1005–1025. https://doi.org/10.5194/bg-4-1005-2007.

Massad, R.S., Nemitz, E., Sutton, M.A., 2010. Review and parameterisation of bi-directional ammonia exchange between vegetation and the atmosphere. Atmos. Chem. Phys. 10 (21), 10359–10386. https://doi.org/10.5194/acp-10-10359-2010.

Mosquera, J., Hensen, A., Van Den Bulk, W.C.M., Vermeulen, A.T., Erisman, J.W., 2001. Long term NH_3 flux measurements above grasslands in the Netherlands. Water Air Soil Poll. 1, 203–212.

Oenema, J., Burgers, S., van Keulen, H., van Ittersum, M., 2015. Stochastic uncertainty and sensitivities of nitrogen flows on dairy farms in The Netherlands. Agric. Syst. 137, 126–138. https://doi.org/10.1016/j.agsy.2015.04.009.

Parkin, T.B., Venterea, R.T., Hargreaves, S.K., 2012. Calculating the detection limits of chamber-based soil greenhouse gas flux measurements. J. Environ. Qual. 41 (3), 705–715. https://doi.org/10.2134/jeq2011.0394.

Pedersen, A.R., Petersen, S.O., Schelde, K., 2010. A comprehensive approach to soil-atmosphere trace-gas flux estimation with static chambers. Eur. J. Soil Sci. 61 (6), 888–902. https://doi.org/10.1111/j.1365-2389.2010.01291.x.

Post, P.M., Hogerwerf, L., Bokkers, E.A., Baumann, B., Fischer, P., Rutledge-Jonker, S., de Boer, I.J., 2020. Effects of Dutch livestock production on human health and the environment. Sci. Total Environ. 737, 139702. https://doi.org/10.1016/j.scitotenv.2020.139702.

R Core Team (2024). R: A Language and Environment for Statistical Computing. R Foundation for Statistical Computing, Vienna, Austria. ⟨https://www.R-project.org/⟩.

Richardson, K., Steffen, W., Lucht, W., Bendtsen, J., Cornell, S.E., Donges, J.F., Rockström, J., 2023. Earth beyond six of nine planetary boundaries. Sci. Adv. 9 (37), eadh2458. https://doi.org/10.1126/sciadv.adh2458.

Rumburg, B., Mount, G.H., Yonge, D., Lamb, B., Westberg, H., Filipy, J., Johnson, K., 2006. Atmospheric flux of ammonia from sprinkler application of dairy waste. Atmos. Environ. 40 (37), 7246–7258. https://doi.org/10.1016/j.atmosenv.2006.04.034.

Sintermann, J., Neftel, A., Ammann, C., Häni, C., Hensen, A., Loubet, B., Flechard, C.R., 2012. Are ammonia emissions from field-applied slurry substantially over-estimated in European emission inventories? Biogeosciences 9 (5), 1611–1632.

Spirig, C., Flechard, C.R., Ammann, C., Neftel, A., 2010. The annual ammonia budget of fertilised cut grassland–Part 1: Micrometeorological flux measurements and emissions after slurry application. Biogeosciences 7 (2), 521–536. https://doi.org/10.5194/bg-7-521-2010.

Stevens, C.J., 2019. Nitrogen in the environment. Science 363 (6427), 578–580. https://doi.org/10.1126/science.aav8215.

Stokstad, E., 2019. Nitrogen crisis threatens Dutch environment—and economy. Science 366 (6470), 1180–1181. https://doi.org/10.1126/science.366.6470.1180.

Stolk, P.C., Jacobs, C.M.J., Moors, E.J., Hensen, A., Velthof, G.L., Kabat, P., 2009. Significant non-linearity in nitrous oxide chamber data and its effect on calculated annual emissions. Biogeosci. Discuss. 6 (1), 115–141. https://doi.org/10.5194/bgd-6-115-2009.

Sutton, M.A., Burkhardt, J.K., Guerin, D., Nemitz, E., Fowler, D., 1998a. Development of resistance models to describe measurements of bi-directional ammonia surface–atmosphere exchange. Atmos. Environ. 32 (3), 473–480. https://doi.org/10.1016/S1352-2310(97)00164-7.

Sutton, M.A., Milford, C., Dragosits, U., Place, C.J., Singles, R.J., Smith, R.I., Wyers, G.P., 1998b. Dispersion, deposition and impacts of atmospheric ammonia: quantifying local budgets and spatial variability. Environ. Pollut. 102 (1), 349–361. https://doi.org/10.1016/S0269-7491(98)80054-7.

Thompson, R.B., Meisinger, J.J., 2005. Gaseous nitrogen losses and ammonia volatilization measurement following land application of cattle slurry in the mid-Atlantic region of the USA. Plant Soil 266, 231–246.

Todd, R.W., Cole, N.A., Rhoades, M.B., Parker, D.B., Casey, K.D., 2011. Daily, monthly, seasonal, and annual ammonia emissions from Southern High Plains cattle feedyards. J. Environ. Qual. 40 (4), 1090–1095. https://doi.org/10.2134/jeq2010.0307.

Tulp, T., Tietema, A.T., van Loon, E.E., Ebben, B., van Hall, R.L., van Son, M., Barmentlo, S.H., 2024. Biomonitoring of dairy farm emitted ammonia in surface waters using phytoplankton and periphyton. Sci. Total Environ. 908, 168259. https://doi.org/10.1016/j.scitotenv.2023.168259.

Van Damme, M., Clarisse, L., Dammers, E., Liu, X., Nowak, J.B., Clerbaux, C., Flechard, C.R., Galy-Lacaux, C., Xu, W., Neuman, J.A., Tang, Y.S., Sutton, M.A., Erisman, J.W., Coheur, P.F., 2015. Towards validation of ammonia (NH 3) measurements from the IASI satellite. Atmos. Meas. Tech. 8 (3), 1575–1591.

van der Molen, J., Van Faassen, H.G., LeClerq, M.Y., Vriesema, R., Chardon, W.J., 1990. Ammonia volatilization from arable land after application of cattle slurry. 1. Field estimates. Neth. J. Agric. Sci. 38, 145–158.

van der Weerden, T.J., Jarvis, S.C., 1997. Ammonia emission factors for N fertilizers applied to two contrasting grassland soils. Environ. Poll. 95 (2), 205–211.

van Weerdenburg, R., Pearson, S., van Prooijen, B., Laan, S., Elias, E., Tonnon, P.K., Wang, Z.B., 2021. Field measurements and numerical modelling of wind-driven exchange flows in a tidal inlet system in the Dutch Wadden Sea. Ocean Coast. Manag 215, 105941. https://doi.org/10.1016/j.ocecoaman.2021.105941.

Weber, A., Khalil, I.M., Schraml, M., Gutser, R., 2018. Soil-atmosphere exchange of NH_3 and NO_x in differently managed vegetation types of Southern Germany. J. Soil Plant Biol. 1 115. https://doi.org/10.33513/JSPB.

Wong, C.L., 2018. Analysis of the number of flux chamber samples and study area size on the accuracy of emission rate measurements. J. Air Waste Manag. Assoc. 68 (10), 1103–1117. https://doi.org/10.1080/10962247.2018.1469555.

Wright, M.N., Ziegler, A., 2017. ranger: a Fast Implementation of Random Forests for High Dimensional Data in C++ and R. J. Stat. Softw. 77 (1), 1–17. https://doi.org/10.18637/jss.v077.i01.

Zhang, Q., Li, Y., Wang, M., Wang, K., Meng, F., Liu, L., Zhao, Y., Ma, L., Zhu, Q., Xu, W., Zhang, F., 2021. Atmospheric nitrogen deposition: a review of quantification methods and its spatial pattern derived from the global monitoring networks. Ecotoxicol. Environ. Saf. 216, 112180. https://doi.org/10.1016/j.ecoenv.2021.112180.